Proceedings Article

Preventing interference between saturation coil and receive coil in MPI

Ege Kor [a,b,*] · Musa Tunç Arslan [a,b,c] · Manouchehr Takrimi [b] · Emine Ulku Saritas [a,b]

[a]Department of Electrical and Electronics Engineering, Bilkent University, Ankara, Turkey
[b]National Magnetic Resonance Research Center (UMRAM), Bilkent University, Ankara, Turkey
[c]Computational Radiology Laboratory, Department of Radiology, Harvard Medical School, Boston, Massachusetts, USA
*Corresponding author, email: ege.kor@bilkent.edu.tr

Abstract

In magnetic particle imaging (MPI), the signals received from magnetic nanoparticles (MNPs) are directly proportional to concentration. Hence, accumulation of MNPs in off-target organs may overpower the signal from actual regions-of-interest that contain MNPs at a smaller concentration. We previously proposed placing a saturation coil over the off-target organ to locally suppress its signal. However, the saturation coil caused a large interference signal on the receive coil, necessitating the acquisition of a separate baseline to determine the interference signal. In this work, we propose methods to prevent the interference between the saturation coil and the receive coil to enable localized signal suppression without the need for an additional baseline acquisition.

I. Introduction

Magnetic nanoparticles (MNPs) that are used as imaging tracers in magnetic particle imaging (MPI) [1, 2] are typically processed in organs such as liver and spleen, and hence can accumulate in these off-target organs [3–5]. Because the pixel intensity in MPI is directly proportional to the concentration of MNPs and the imaging point spread function PSF is relatively wide [6], the high signal from these off-target organs may overpower or obscure the low signals from the actual target regions of interest (ROIs).

One approach to alleviate this problem is to increase the resolution by utilizing higher selection field gradients or MNPs with larger diameters. However, using higher gradients reduces the size of the field-of-view (FOV) [4, 6], and using larger MNPs results in increased relaxation blur [7]. We recently proposed placing a saturation coil over the off-target organs where MNPs accumulate to suppress the signal from these regions [8]. However, saturation coil generated an interference on the receive coil and dominated the received signal, necessitating the acquisition of an additional baseline signal with the saturation coil placed inside the MPI scanner. In this work, we propose methods to obviate the need for an additional baseline measurement when using a saturation coil. We demonstrate on our field free line (FFL) MPI scanner that utilizing a choke inductor together with the saturation coil can successfully prevent the interference, enabling higher quality images with localized signal suppression capability.

II. Materials and Methods

II.I. Saturation Coil and Interference

During the experiments, a saturation coil is placed around a chosen region of the phantom, with a DC current passing through the coil to locally saturate the
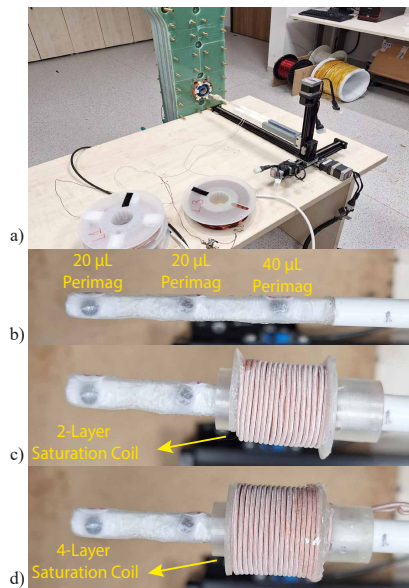
Figure 1: (a) In-house FFL MPI scanner and the experiment setup. (b) Imaging phantom containing three samples of Perimag MNPs at different volumes. (c) 2-layer saturation coil and (d) 4-layer saturation coil, placed over the 40 μL Perimag sample to locally suppress its signal.

MNP magnetization. As shown in Fig.1, a linear actuator moves the phantom together with the saturation coil, along the z-direction inside the bore of our FFL scanner. However, the drive field (DF) induces currents on the saturation coil, which in turn induces an interference signal on the receive coil. This interference signal is both large and position-dependent, necessitating an additional baseline signal to be acquired. During this baseline acquisition, the saturation coil is moved inside the scanner exactly as in the imaging experiment, but without the phantom.

To reduce the induced currents on the saturation coil, we propose increasing the impedance of the overall saturation coil setup at the DF frequency. Here, we consider two different approaches: placing an additional resistor or a choke inductor in series with the saturation coil. For the first approach, a maximum of 3 Ω resistor could be utilized due to the power limits of the DC current source. Adding this resistor effectively increased the impedance of the overall saturation coil setup by 2- to 3-fold. For the second approach, a choke inductor with 27 mH inductance was implemented. An air core was utilized due to the large DC currents passing through the choke, as magnetic cores suffer from hysteresis effects under DC fields. The DC resistance of the choke was about 3 Ω, with a condirably large impedance of 2.05 kΩ at the 12.1 kHz DF frequency of our MPI scanner. Hence, the choke was designed to allow DC current needed for signal saturation, but block the AC current to prevent induction at the DF frequency.
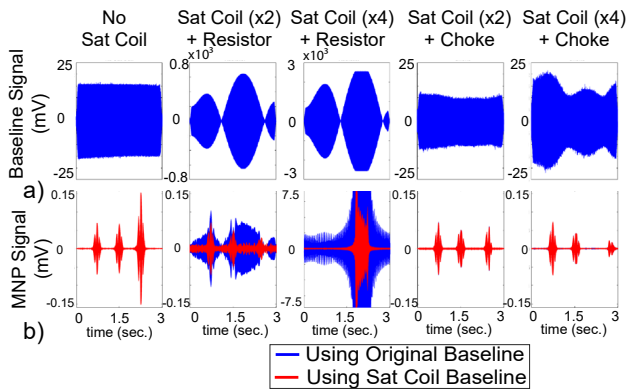
II.II. Saturation Coil Design

Two separate saturation coils were designed, as shown in Fig. 1(c)-(d). One of the saturation coils had 2 layers of windings with 2 cm outer diameter, and the other one had 4 layers of windings with 2.5 cm outer diameter. The coil sensitivities were 1.39 mT/A and 2.63 mT/A for the 2- and 4-layer saturation coils, respectively. The inductances for these coils were 12.3 μH and 46.0 μH, and the impedances at the 12.1 kHz DF frequency were 1.4 Ω and 3.6 Ω, respectively. Note that the impedance of the choke inductor was three orders of magnitude larger than these impedances, enabling a significant reduction of the currents induced on the saturation coil. Common parameters were: 1.5 cm inner diameter, 16 windings per layer, wounded using a 1.2 mm diameter Litz wire. During imaging, 20 A DC was applied through the saturation coils, creating 27.8 mT and 52.6 mT DC field for 2- and 4-layer saturation coils, respectively. While this relatively large DC current may normally require a cooling strategy, no significant heating issues were observed for the short scan times (approximately 3 seconds) used in the imaging experiments.

II.III. Imaging Experiments

The imaging experiments were conducted on our in-house FFL MPI scanner shown in Fig.1(a). The selection field gradients were (-4.4, 0, 4.4) T/m in (x, y, z) directions. The DF was applied at 12.1 kHz and 10 mT along the z-direction. The free imaging bore diameter of the scanner was 3.5 cm. Images were acquired in a 1D FOV of 9.1 cm along the z-direction. The linear actuator moved at a speed of 3 cm/sec. The total scan time was approximately 3 sec. As shown in Fig.1(b), the imaging phantom contained 3 samples: two samples with 20 μL each, and a third high-signal sample with 40 μL to mimic the off-target accumulation organ. All samples contained Perimag MNPs with 17 mg Fe/mL undiluted concentration. The center-to-center distances between the samples were 2.3 cm along the z-direction.

Five different imaging experiments were performed. In the first experiment, the phantom was imaged without the saturation coil. In the second and third experiments, a 3 Ω resistor was used together with the 2- and 4-layer saturation coils, respectively. In the fourth and fifth experiments, a 27 mH choke was used together with the 2- and 4-layer saturation coils, respectively. In each experiment, the baseline signal and the received signal for the phantom were measured separately. For the cases when a saturation coil was used, a second baseline signal was acquired as described before to determine the interference signal.

The signals were amplified with a low-noise pre-amplifier (LNA) (SRS SR560), and digitized using a data acquisition card (NI USB-6383). MNP signals were obtained by subtracting the baseline signal from the re-
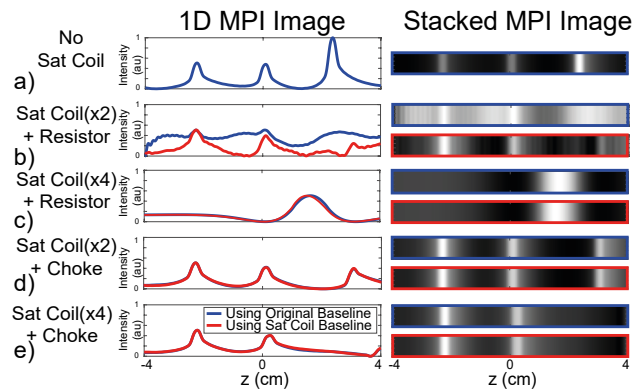
Figure 2: (a) Baseline signal without and with saturation coils. (b) MNP signal, formed by subtraction of baseline signal from the received signal, followed by direct feedthrough filtering. Using the original baseline (i.e., without the saturation coil) is compared with using the baseline with the saturation. The signals are plotted after normalization by the respective LNA gains.

Figure 3: 1D MPI images and their 2D stacked versions (a) without saturation coil, (b) with 2-layer saturation coil together with a resistor, (c) with 4-layer saturation coil together with a resistor, (d) with 2-layer saturation coil together with a choke, and (e) with 4-layer saturation coil together with a choke.

ceived signal, followed by direct feedthrough filtering to remove the fundamental harmonic. Images were reconstructed using x-space based Partial FOV Center Imaging (PCI) algorithm [9].

III. Results and Discussion

Figure 2 shows the baseline signals and MNP signals of all five experiments, and Fig. 3 displays the corresponding 1D MPI image profiles and their 2D stacked versions. In Fig. 2(a), when the 2-layer saturation coil is used together with the resistor, the interference signal limited the LNA gain to a maximum of 5. When the 4-layer saturation coil is used together with the resistor, the interference signal further increases in amplitude and overloads the LNA even at a gain of 2. In contrast, when the saturation coils are used together with the choke, the interference signal is significantly reduced and the LNA gain can be set to 100. For the baseline signals in Fig. 2(a), the root mean square (RMS) values were 8.6 mV for the case of no saturation coil, 0.26 V and 1.19 V for the cases of using a resistor together with 2-layer and 4-layer saturation coils respectively, and 5.1 mV and 7.0 mV for the cases of using a choke together with 2-layer and 4-layer saturation coils respectively. These values indicate that utilizing a choke together with the saturation coil successfully prevents the formation of undesired interferences. Figure 2(b) compares the MNP signal when the baseline without or with saturation coil is used during baseline subtraction. These results show that using the saturation coil together with a choke preserves the MNP signal quality.

The MPI images in Fig. 3(b) demonstrate that, when using a resistor is used to prevent interference, a separate baseline with the saturation coil is still needed. Further-

more, for the case of the 4-layer saturation coil in Fig. 3(c), a separate baseline does not suffice and the image cannot be reconstructed successfully due to the extremely strong interference. In contrast, as shown in Fig. 3(c)-(d), the original baseline (i.e., without saturation coil) is sufficient when using a choke to prevent interference. When the 2- and 4-layer saturation coils are compared, one can see that the 4-layer saturation coil achieves complete suppression of the high-signal MNP target, thanks to its larger DC field.

In Fig. 3, for the cases where the saturation coil is used, a slight decrease in signal together with a slight shift in position can be observed for the middle sample of the phantom. This change in signal is potentially due to the relatively small but non-zero DC field from the saturation coil. For the 2-layer saturation coil, the DC fields experienced by the middle and left samples were 1.2 mT and 0.2 mT, respectively. For the 4-layer saturation coil, the respective values were 2.6 mT and 0.4 mT.

In an in vivo setting, the signal from a high concentration region may completely overpower the signal from low concentration ROIs due to the relatively wide PSF in MPI. While the saturation coil can successfully suppress the signal from a high concentration region, this work shows that the interference signal due to the saturation coil could also obscure the MNP signal from low concentration ROIs. Therefore, preventing the formation of this interference is a crucial step for imaging low concentration ROIs.

IV. Conclusion

In this study, we proposed using a choke inductor together with a saturation coils to locally suppress MNP signal while preventing undesired interference on the receive coil. With this setup, a separate baseline for de-

termining the interference due to the saturation coil is no longer needed, and the significantly reduced interference levels enable the usage of high LNA gain. The experimental results on our FFL scanner demonstrate successful localized suppression of high-signal MNP regions, while maintaining signal quality.

Acknowledgments

Author's statement

Conflict of interest: Authors state no conflict of interest.

References

[1] B. Gleich and J. Weizenecker. Tomographic imaging using the nonlinear response of magnetic particles. *Nature*, 435:1214–7, 2005, doi:10.1038/nature03808.

[2] N. Talebloo, M. Gudi, N. Robertson, and P. Wang. Magnetic particle imaging: Current applications in biomedical research. *Journal of Magnetic Resonance Imaging*, 51(6):1659–1668, 2020, doi:https://doi.org/10.1002/jmri.26875.

[3] Z. W. Tay, P. Chandrasekharan, A. Chiu-Lam, D. W. Hensley, R. Dhavalikar, X. Y. Zhou, E. Y. Yu, P. W. Goodwill, B. Zheng, C. Rinaldi, and S. M. Conolly. Magnetic particle imaging-guided heating in vivo using gradient fields for arbitrary localization of magnetic hyperthermia therapy. *ACS Nano*, 12(4):3699–3713, 2018, PMID: 29570277. doi:10.1021/acsnano.8b00893.

[4] E. U. Saritas, P. W. Goodwill, L. R. Croft, J. J. Konkle, K. Lu, B. Zheng, and S. M. Conolly. Magnetic particle imaging (mpi) for nmr and mri researchers. *Journal of Magnetic Resonance*, 229:116–126, 2013, Frontiers of In Vivo and Materials MRI Research. doi:https://doi.org/10.1016/j.jmr.2012.11.029.

[5] P. W. Goodwill, E. U. Saritas, L. R. Croft, T. N. Kim, K. M. Krishnan, D. V. Schaffer, and S. M. Conolly. X-space mpi: Magnetic nanoparticles for safe medical imaging. *Advanced Materials*, 24(28):3870–3877, 2012, doi:https://doi.org/10.1002/adma.201200221.

[6] P. W. Goodwill and S. M. Conolly. Multidimensional x-space magnetic particle imaging. *IEEE Transactions on Medical Imaging*, 30(9):1581–1590, 2011, doi:10.1109/TMI.2011.2125982.

[7] Z. W. Tay, D. W. Hensley, E. C. Vreeland, B. Zheng, and S. M. Conolly. The relaxation wall: Experimental limits to improving mpi spatial resolution by increasing nanoparticle core size. *Biomedical Physics & Engineering Express*, 3(3):035003, 2017, doi:10.1088/2057-1976/aa6ab6.

[8] E. Kor, M. T. Arslan, and E. U. Saritas. Saturation coil for localized signalsuppression in mpi. *International Journal on Magnetic Particle Imaging*, 8(1), 2022, doi:10.18416/IJMPI.2022.2203013.

[9] S. Kurt, Y. Muslu, and E. U. Saritas. Partial fov center imaging (pci): A robust x-space image reconstruction for magnetic particle imaging. *IEEE Transactions on Medical Imaging*, 39(11):3441–3450, 2020, doi:10.1109/TMI.2020.2995410.